I NTROCDUCTION

Calcium phosphate glasses are extensively studied in recent years because they can be bioactive materials. For example, phosphate glasses containing large amounts ofcalcium are able to bind to bone and therefore can be used as versatile materials for implants. It is posible to create phosphate glasses with high CaO content to be close to the chemical composition of bone.

This paper aims in the first part is to study the changes that occur in the structure glasses based on P_2O_5 and CaO (at a rate of 1-1) with addition of other oxides like: Ag_2O, Au_2O_3 and K_2O, and on the other hand, their behavior in two environments: one with composition similar to human blood (simulated body fluid SBF) and the second in a bacterial environment. By introducing the samples in SBF to study their ability to form hydroxyapatite and can be used as biomaterials for different implants. Environmental bacterial behavior study in contact with this glasses (or liquids containing these glasses) offers the opportunity to create some material or liquids containing such glasses with an tibacterial properties.

The thesis is structured in four chapters.

The first chapter covers the general notions of phosphate glasses, the raw materials used in obtaining them, methods for obtaining vitreous materials and applications of glasses. Here we find the structure of phosphorus pentoxide glasses and structure of binary glasses containing P_2O_5 and CaO.In the second and third chapter, based on data from the literature are presented theoretical and experimental methods used in study of structure and properties ofoxide glasses: X-ray diffraction, IR absorption spectroscopy, Raman effect and differential thermal analysis (DTA) . Also in Chapter 3 describes how were prepared the studied glasses.

In the forth chapter are presented and disscused the experimantal results obtained for the investigated glasses. In the end are presented the general conclusions which evidenced the most important results of this thesis.

Keywords: *glasses, x-ray Diffraction, FT – IR spectroscopy, Raman spectroscopy,Diferential thermal analysis,Ssimulated body fluid;Antibacterial efect*

Chapter I - The structure of phosphate glasses, methods of obtaining and some applications of vitreous oxide materials

The common oxidic glass is known fron the antiquity, being used as constructions material, as art objects, as adornments, as electronic materials , as biomaterials, absorbent shield in nuclear technique, in photographic technique, etc., with applicability in so many other domains.

Oxidic glasses are a part of non-crystalline solid materials in which the atoms are disposed in a way similar to the crystals, but their arrangement is not regular, presenting only local order. In order to obtain glasses there is a large number of oxide species known as vitreous network forming (SiO_2, B_2O_3, P_2O_5, GeO_2, TeO_2, V_2O_5, Bi_2O_3, etc.). The other oxides which enter in the chemical composition of the glasses, stabilizing it and modifying its properties have been named vitreous network modifier or stabilizer oxides (K_2O, CaO, Na_2O, CdO, SrO, Li_2O, etc.).

Phosphorus is pentavalent because one of the electrons can pass from 3s to 3d orbital whose energy level is very high, resulting in a hybridization sp3d. Therefore in PO_4 tetrahedron the 4 links P – O are not equivalent, one being short, having double bond character while π and chemically inactive. Average distance is 1.55 A, simple links and 1.39A for the double.

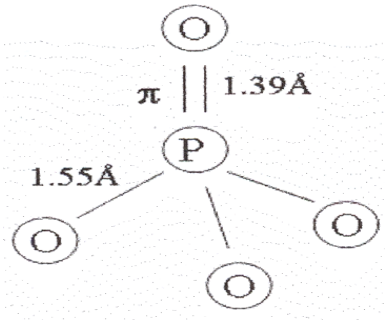

Figura 1.1 Structural units PO_4

P_2O_5 is found in three crystalline forms, and all three contain [PO4] thetraedra : hexagonal, consisting of P_4O_{10} molecules linked by Van der Waals forces (Fig. 1.2), orthorhombic cycles consisting of 10 tetrahedrons, tetragonal structure consist of stratified 6 tetrahedra.

.

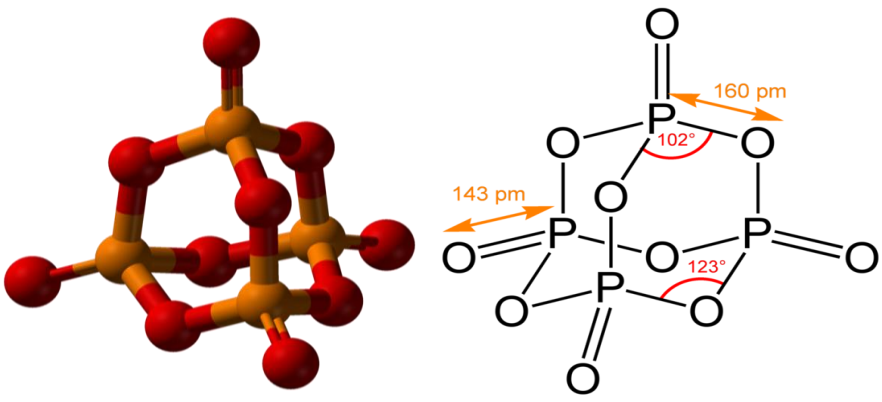

Figura 1.2 Structural units that exist in P_2O_5

Adding different modifiers (PbO, Na_2O, K_2O, etc) in B_2O_3 glasses, it can be obtain binary glasses in which the modifier determines structural changes, complicating even more the structure of these glasses [3-5]. The increasing of alkaline oxide concentration determines not only the increasing of phosphorous coordination, but also the breaking of dome oxygen bridges which leads to depolimerization.

The introduction of a third component in P_2O_5 based glasses complicates even more the structure of these glasses and the investigation of their structure and properties. Analizing the structure of ternary phosphate glasses is more complicated than binary phosphate glasses and starts with analizing th structure of the binary phosphate glasses. In this paper the components which are present in chemical composition of phosphatw glasses are CaO, Ag_2O, Au_2O_3 and K_2O.

The introduction of transitional metal ions the glasses special electrical and magnetical properties and at the same time they are used as check rod for investigating the structure of these glasses.

Capter II. Methods of study on the structure of vitreous oxide materials

Studying oxidic glasses with transitional metal ions has as ajective the gathering of information regarding their structure and their properties, in order to contribute in the elaboration of vitreous solid theory and finding new practically applications. The investigation methods used for this study are X – ray diffraction, FT – IR spectroscopy, Raman spectroscopy.

X – Ray diffraction is the most used investigation method in order to establish if a material is crystalline, vitreous or amorphous. In order to do this you have to obtain the X-ray diffraction image and to know how the destruction of crystalline state affects the diffraction image.

FT – IR spectroscopy is used in crystalline and in non-crystalline materials studies, being one of the most used methods for investigating the molecular structure and for qualitative and quantitative analysis of substances. The structure of the IR absorption spectrum gives us information regarding the geometrical

properties of the molecule (distances between atoms, valence angles, and force constants) and its chemical structure.

The Raman spectroscopy, complementary to IR spectroscopy, brings useful contributions to the molecular vibrations study. Comparing with FT-IR spectra, the Raman spectra has a number of advantages : the bands are, generally, well-defined; limited in numbers and often polarized; they have a strong dependence of composition; with a small sensibility to surface contamination and water content; the samples permit volume effects measurements; measuring at high temperatures is a lot easier.

Chapter III. Experimental techniques

The raw materials used in the preparation of the investigated glasses are: $AgNO_3$, $(NH)_4\,H_2PO_4$, $AuCl_3$, $KCaO_3$ şi $CaCO_3$ These materials were mixed in stoechiometric proportions given by chemical formula for $xAg_2O\cdot$ (100-x)[$P_2O_5\cdot CaO$] cu x=0; 0.3;0.5;1, 5%mol ; $xK_2O\cdot$ (100-x)[$P_2O_5\cdot CaO$] cu x=0; 0.3;0.5;1; 5; 10; 20; 35, 50%mol; $xAu_2O_3\cdot$ (100-x)[$P_2O_5\cdot CaO$] cu x=0; 0,3; 0,5; 1, 3%mol and melted at 1250 ˚C in aluminum crucible for a half an hour to achieve better homogenization. In order to obtain a vitreous structure, the melt was cooled on a plate of stainless steel (melt cooling method).

The structure of samples was analyzed by means of x-ray Diffraction, using powders. To confirm the data obtained from these measurements was also used the scanning electron microscopy method.

The FT – IR spectra have been recorded using a Bruker Equinox 55 with a spectral range from 4000 cm^{-1} to 370 cm^{-1}. A MIR, GLOBAR generator cooled with air was used. The detection was carried out with a DLATGS detector with a KBr window. The spectral resolution was about 0.5 cm^{-1}. The samples were prepared using KBr pellet technique.

Raman measurements were made with a Dilor Labram spectrometer (invers system, HRLabRam, Jobin Yvon Horiba) using using the 1064 nm line of a Nd/YAG laser. The power of the laser was 5 mW. The signal acquisition has been done using a CCD (Peltier CCD) and the soft was LabSpec 3.1. The spectra were obtained from 8 cycles of 30 seconds average, and the spectral resolution was 1 cm^{-1}.

Capter. IV. Results and discussion obtained on the structure, bioactive and antibacterial proprieties of some phosphate glasses

4.1. Structural characterization on $xAg_2O\cdot(100-x)[P_2O_5\cdot CaO]$ glass system

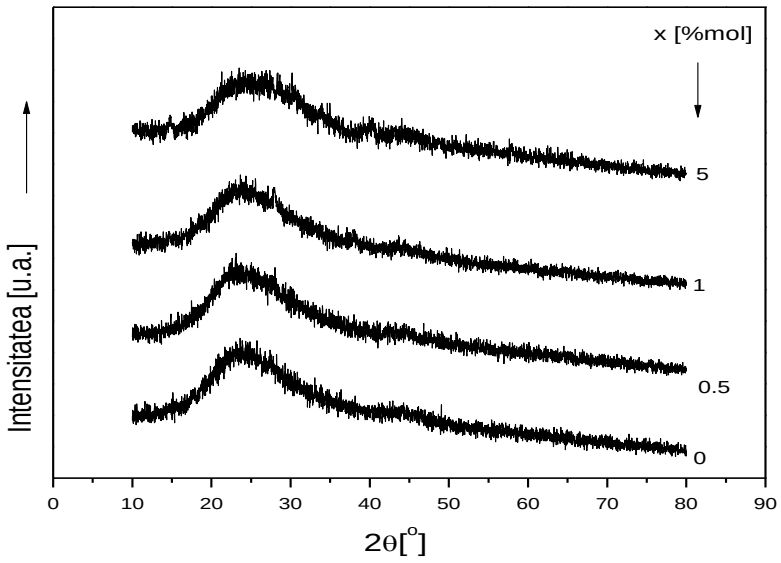

Figura 4.1 X-ray diffractograms of $xAg_2O\cdot(100-x)[P_2O_5\cdot CaO]$ glass system with $0\leq x\leq 5$mol%

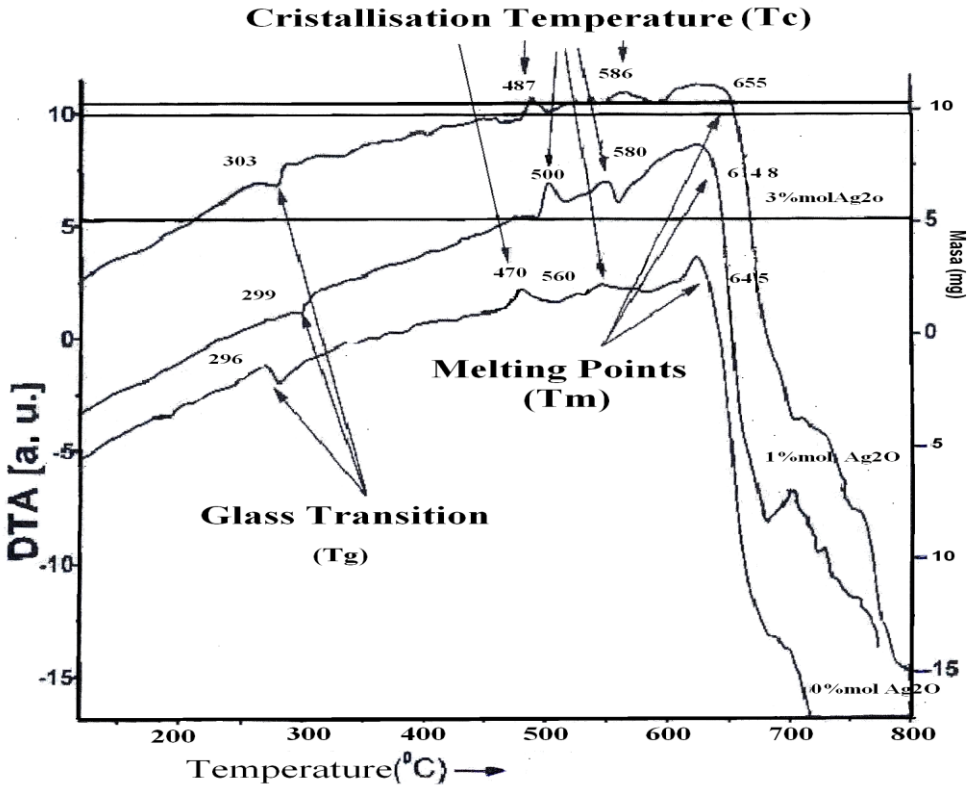

Figura 4.2 DTA and TGA of $xAg_2O\cdot(100-x)[P_2O_5\cdot CaO]$ glass system x=0; 1 and 3%mol

IR spectra of P_2O_5·CaO glass matrix reveals in the first part of spectral range two large bands : ~ 500 cm^{-1} assigned to the fundamental O=P-O bending vibrations and ~ 752 cm^{-1} corresponding to symmetric stretching vibrations of P-O-P [3,4].

In the 800-1300 cm^{-1} spectral region we found vibrations of P-O-P bonds linked with linear metaphosphate chain (~ 912 cm^{-1}) and asymmetric stretch of P=O (~ 1280 cm^{-1}) [3,5].

The band from ~ 1112 cm^{-1} can be associated with symmetric stretching $(PO_2)^-$ and asymmetric stretching of $(PO_3)^{-2}$ terminal groups [4,6].

For all glasses with $x \leq 1$ mol% appears a weak band at 1400 cm^{-1} attributed to the P-O- correlated to the self network vibrations [3].

IR spectra of glasses shoed a very peak at ~ 1640 cm^{-1} which my be attributed to the bending vibrations of free H_2O molecules [7]. The presence of water molecules in our glasses was probably because the mixtures had absorbed some water during the investigate process.

In addition of Ag_2O a weakening of P=O might be expected with this bond being ruptured by network forming cations. If instead the cation entered the network interstitially as an ion , the network is gradually broken down and new spectral bands may appear corresponding to the vibrational character of free charged structural units. The increasing of Ag_2O content has a result the appearance of two new peaks : ~ 470 cm^{-1} – attributed to the $\delta(PO_2)$ modes of (PO_2) chain groups and ~ 995 cm^{-1} for symmetric stretching of $P\text{-}O^-$ bonds in the $(PO_{3)}^{2-}$ end groups [1].

The partial break down of the covalent vitreous network at high Ag_2O content is show by the weak band at ~ 1112 cm^{-1}, assigned to stretching vibrations of $P\text{-}O^-$ groups, the intensity of this band reaches a fairly strong maximum at 5 mol% [4,6].

It's clearly observed (for 5 mol %) that the intensity of P=O absorption band starts to decrease , we attributed this to the increasing replacement of P=O bonds by P-O-Ag bridging units.

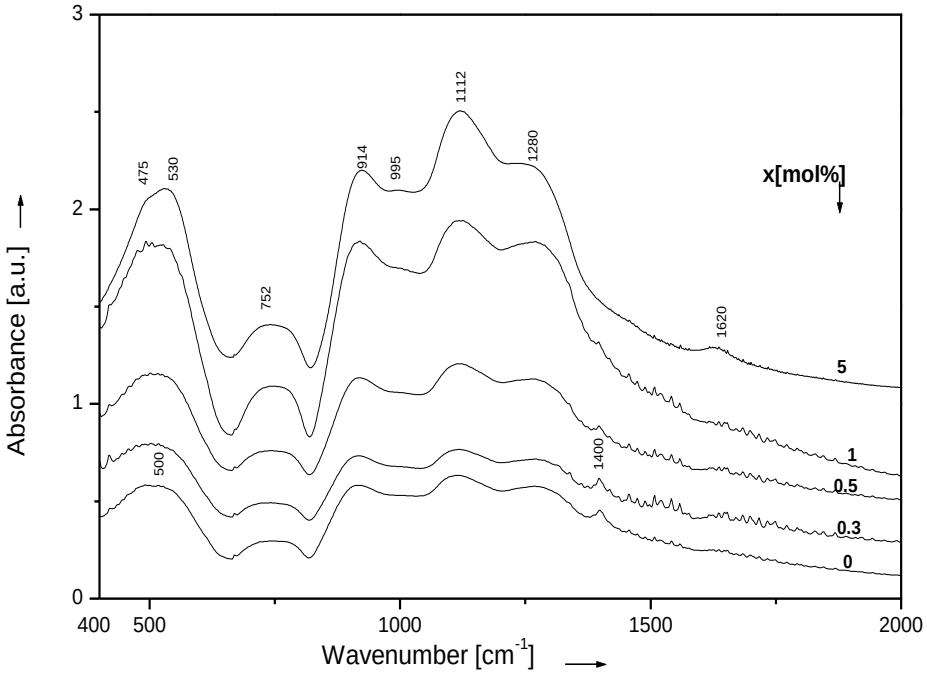

Fig. 1. IR spectra of $xAg_2O\cdot(100-x)[P_2O_5\cdot CaO]$

Fig. 4.3 FT-IR spectra of

x $Ag_2O\cdot(100-x)[P_2O_5\cdot CaO]$ glass system, $0\leq x\leq 5$ %mol

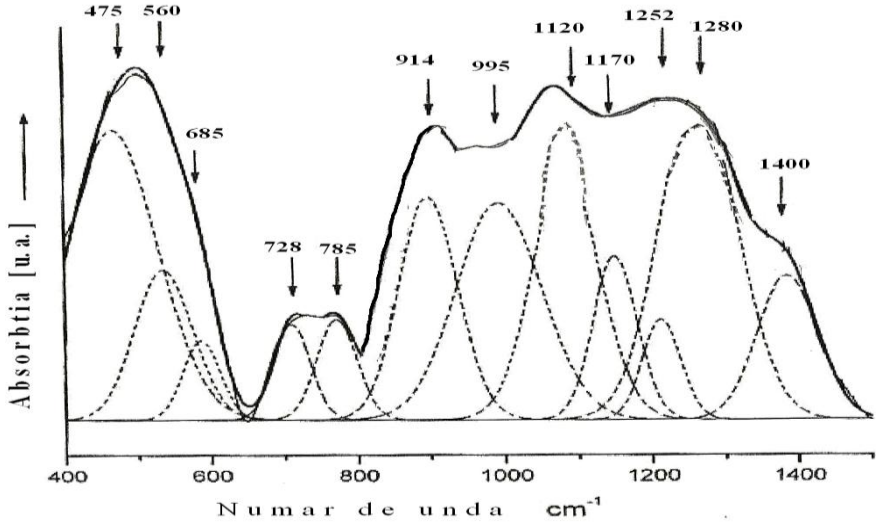

Fig. 4.4 Deconvolution of IR spectra of glass $xAg_2O\cdot(100-x)[P_2O_5\cdot CaO]$ for x=5%mol Ag_2O,

Figure 4.5 shows the Raman spectra of all investigated glasses. There was a two strong bands at ~ 700 cm^{-1} attributed to the symmetric stretching vibrations of P-O-P bonds and ~ 1162 cm^{-1} assigned to the asymmetric stretching vibrations of the $(PO_2)^-$ groups [9,10].

Bues and Gehrke [12] attributed in glass the well defined band observed at ~ 340 cm^{-1} to the PO_2 and chain O-P-O bending vibrations [7,12].

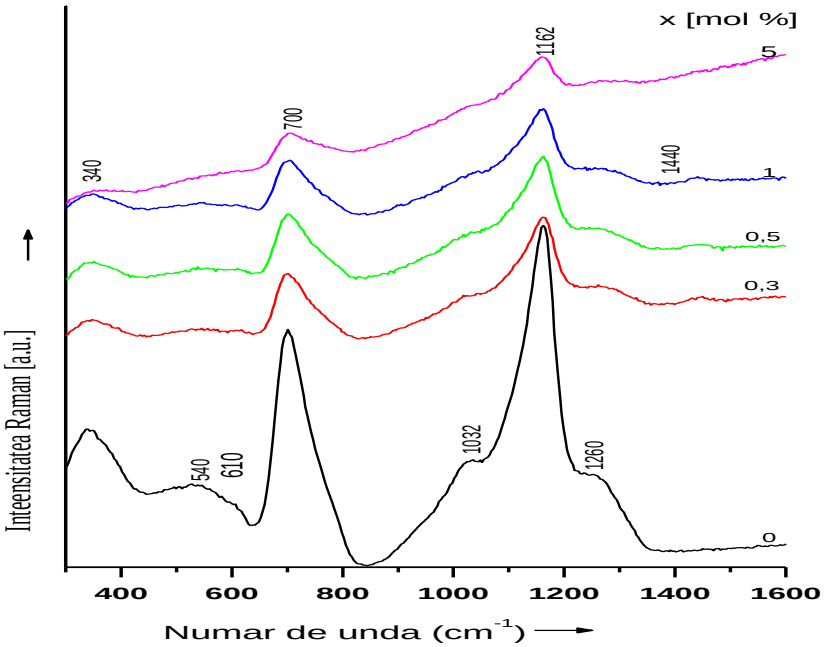

Fig. 4.5 Raman spectra of
$xAg_2O \cdot (100-x)[P_2O_5 \cdot CaO]$ glass system $0 \leq x \leq 5$ %mol

Other bands (two shoulders) appear around 1032 cm^{-1} typical of P_2O_7 group with $\gamma_s(PO_3)$ [13,14,10] and 1250 cm^{-1} due to the vibrations of P=O bonds [10,15].

The large band 450-630 cm^{-1} (centered app. 540 cm^{-1}) belongs to P-O-P chains complex vibrations [8,16]. This band is well observed only for $P_2O_5 \cdot CaO$ glass matrix. Their intensity decrease up to disappearance (when silver oxide is added to the matrix) because of breaking of P-O-P bonds and forming of new P-O- and P-O-Ag bonds.

The decrease in intensity of all this bands with the increase of silver oxide to the glass network matrix concludes the depolimerization process of phosphate glasses structure.

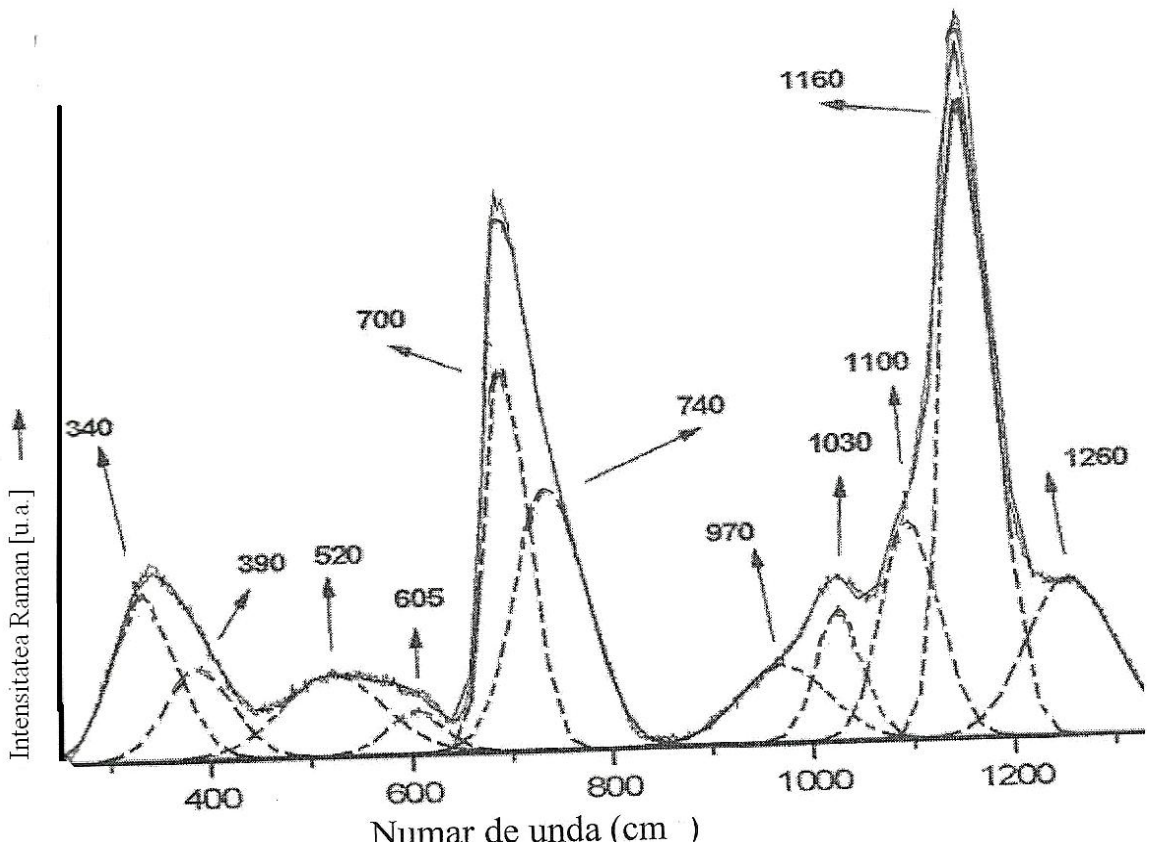

Fig.4.5 Deconvolution of Raman spectra of $xAg_2O\cdot(100\text{-}x)[P_2O_5\cdot CaO]$ glass system, x=0.3 %mol,

4.2. Structural characterization on $xK_2O\cdot(100\text{-}x)[P_2O_5\cdot CaO]$ glass system

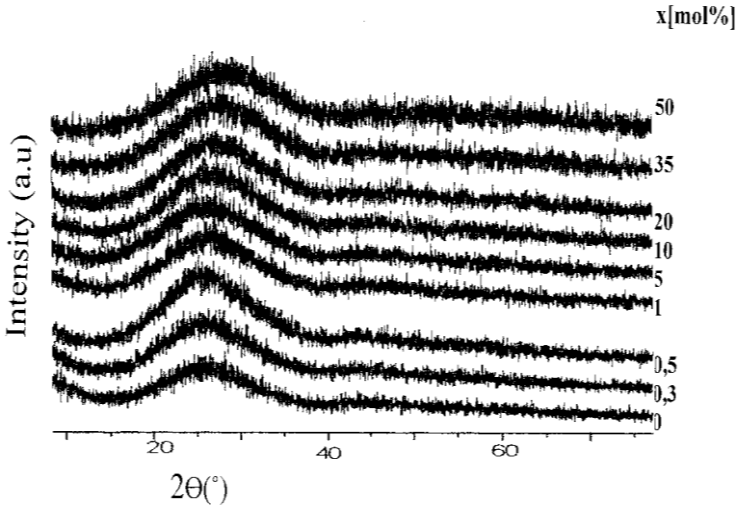

Fig. 4.7 X – ray diffracograms of $xK_2O\cdot(100\text{-}x)[P_2O_5\cdot CaO]$glass system , $0\leq x\leq 50$ %mol

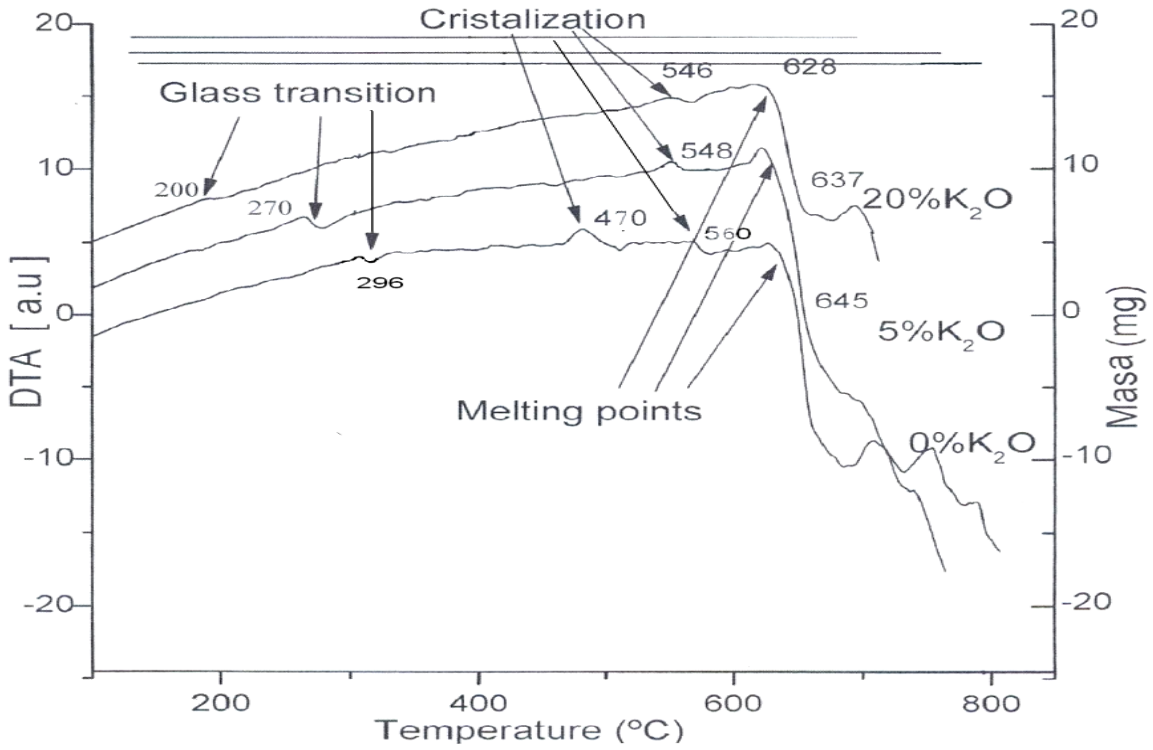

Fig. 4.8 DTA and TGA of

$xK_2O\cdot(100-x)[P_2O_5\cdot CaO]$ glass system cu x=0; 5 and 20%mol

The infrared absorption spectra were obtained for the $xK_2O\cdot(100-x)[P_2O_5\cdot CaO]$ glasses with $0\leq x\leq 50$ mol%. The infrared spectra recorders on investigated samples are present in figure 4.9.The spectra reflect the structural rearrangements of different phosphate structural groups. These groups may connect in several ways increasing the number of allowed vibration modes.

The FT-IR spectra of $[P_2O_5\cdot CaO]$ glass matrix showed bands at: ~520cm^{-1}, ~740cm^{-1}, ~912cm^{-1}, ~1125cm^{-1} , ~1270cm^{-1} and 1640cm^{-1}. The large band with maxim at ~520cm^{-1} is characteristic for the fundamental O=P-O bending vibrations [3, 4]. Bands at ~ 740 cm^{-1} is attributed to a P-O-P stretching vibrations from Q^2 units and peak at ~ 1400 cm^{-1} may be due to a $P\text{-}O^-$ bond stretching vibrations combined with a lattice mode [3,4].

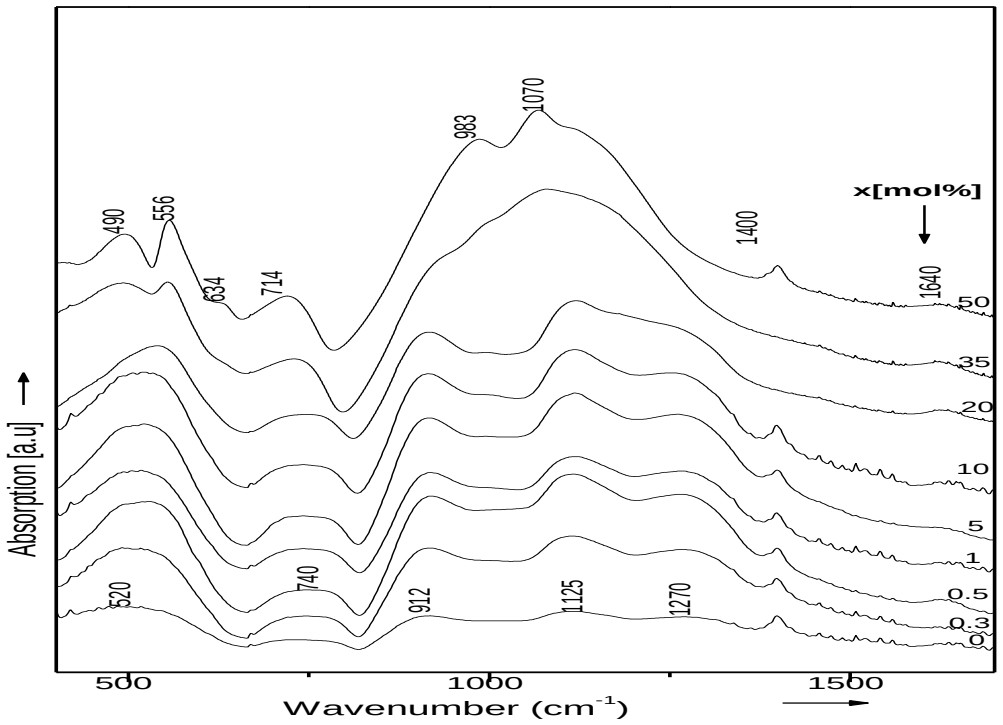

Fig. 4.9 FT-IR specraof $xK_2O\cdot(100\text{-}x)[P_2O_5\cdot CaO]$ glass system, $0\leq x\leq 50$ mol%

We can see that for potassium oxide content greater than 10 mol % the intensity of the P=O (~1270cm^{-1}) absorption band starts to decrease up to the disappearance, we attributed this to the increasing replacement P=O by P-O-K bridging units.

Major changes with the addition of potassium oxide are present in the 850-1300cm^{-1} range, involving the evolution of the intensity and relative area under the absorption bands in this wave number domain especially for 35 mol %. This big large band give evidence of some ionic content in the $xK_2O\cdot(100\text{-}x)[P_2O_5\cdot CaO]$ glass system, the partial break down of the supposedly covalent vitreous network at high potassium oxide content. Also the intensity of this large band reaches a fairly strong maximum for 35 mol% K_2O in the region 1030-1120cm^{-1} when breakdown of the covalent vitreous network into small ionic groups (PO_4^{3-}, $P_2O_7^{4-}$) might expected [11]. To confirm that are bands at ~983 cm^{-1} and at ~1070cm^{-1} which appear at 50 mol % K_2O and have been ascribed to two of normal vibrations modes of the PO_4^{-3} ions, the later band being the symmetrical stretching mode [12,14].

An important remark regards the appearance for high content of potassium oxide a two strong bands: at ~ 490cm^{-1} and at ~556 cm^{-1} associated with symmetric and asymmetric bending mode of the PO_4^{3-} tetrahedral (Q^0) [13,25].

In addition of K_2O a weakening of P=O might be expected with this bond being ruptured by network forming cations. For 50 mol% the phosphate units are more isolated in the structure since in IR absorption spectra appear new bands: ~ 490cm^{-1} and at ~556 cm^{-1} in first part and 983cm^{-1} and 1070cm^{-1} in the second part of spectrum .Finally, a new band peaking at ~634cm^{-1} appears in the IR spectra characteristic to pyrophosphate glasses (Q^1) [15-20].

The evolution of the absorption bands with the increasing of K_2O show the significant distortions of the phosphate groups and concludes the depolymerization process of phosphate glasses structure for maximum content of K_2O.

Table 4.4 FT-IR bands assignment for $xK_2O\cdot(100-x)[P_2O_5\cdot CaO]$ glass system, $0\leq x\leq 50$mol%.

ν (cm^{-1})	Attribution
~490	Symmetric and asymmetric bending mode of the PO_4^{3-} tetrahedral
~520	Bending vibrations of fundamental O=P-O
~556	Symmetric and asymmetric bending mode of the PO_4^{3-} tetrahedral
~714	Asymmetric stretching vibrations of P-O-P linkages
~740	Bending vibrations P-O-P bonds associated to Q^2 units
~912	Asymmetrical bending vibrations of P-O-P bonds
~983 ~1070	Symmetrical stretching vibrations of the PO_4^{3-} ions
~1125	Asymmetrical and symmetrical stretching of PO_3^{2-} (Q^1)
~1270	P=O double stretching bond Q^2 groups
~1400	Stretching vibrations $P\text{-}O^-$ bond combined with a lattice mode
~1640	Bending vibrations of free H_2O molecules

Figure 4.10 shows the Raman spectra of all investigated glasses. For $[P_2O_5\cdot CaO]$ matrix spectra evidence the follow six bands: ~340 cm^{-1}, ~540 cm^{-1}, 1030 cm^{-1}, ~1162 cm^{-1} and ~1250 cm^{-1}.

The most intense band at ~1162 cm^{-1} in the spectrum has attributed to the symmetric and asymmetric stretching vibrations of $(PO_2)^-$ groups from Q^2 units. The less intense band at ~700 cm^{-1} was assigned to the asymmetric stretching vibrations of P-O-P linkages in Q^2 and Q^1 structural units [15, 16].

The large band situated at 400-600 cm^{-1}, with maxim at ~540cm^{-1}, associated with phosphate polyhedral is well observed only for glass matrix and corresponds to the symmetric stretching of P-O- bonds and O-P-O bending modes [11,18]. The intensity of this band decrease up to disappearance because of forming of new units.

Bues and Gehrke [17] attributed in glass metaphosphate the well defined band observed at ~ 340 cm^{-1} to the $(PO_2)^-$ and chain O-P-O bending vibrations.

Other bands (two shoulders) appear at ~ 1030 cm^{-1} typical of P_2O_7 group with $\gamma_s(PO_3^{2-})$ and ~1250 cm^{-1} due to the asymmetric vibrations of P=O bonds existed in Q^2 groups [16,19].

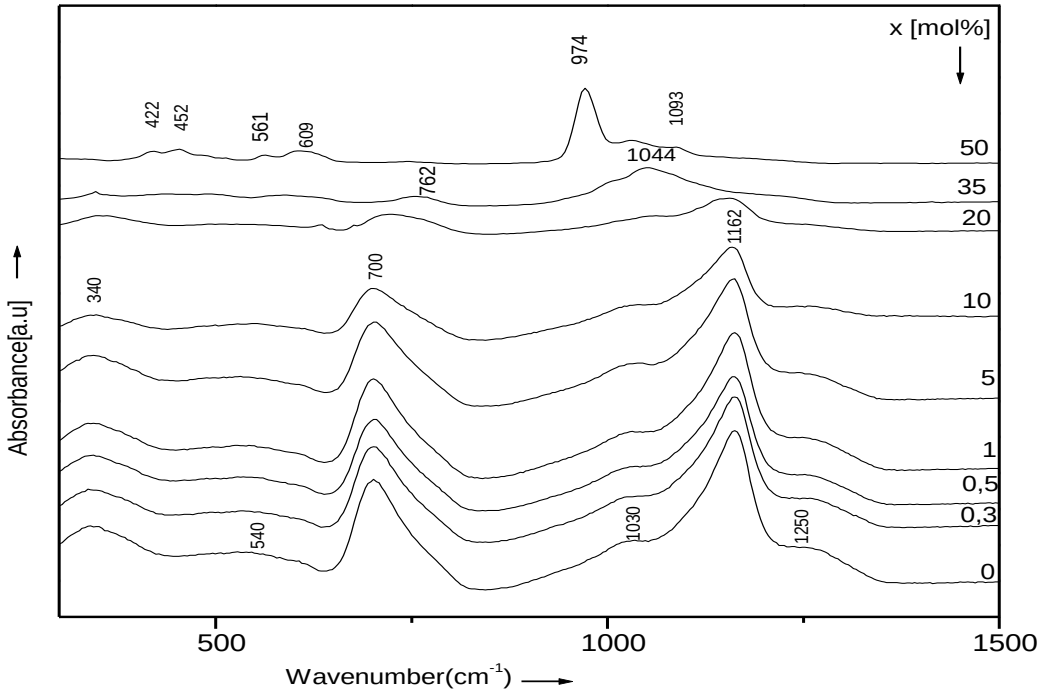

Fig. 4.10. Raman spectra of $xK_2O\cdot(100-x)[P_2O_5\cdot CaO]$ glass system

The intensity of the strong band at ~1160 cm^{-1} decrease with increasing potassium content and almost vanish at x=35mol%. Similar behavior shows the band presented at ~700 cm^{-1}. These changes are accompanied by appearance of new bands at ~1044 cm^{-1} and ~762 cm^{-1} assigned to (PO_3^{2-}) symmetric stretching (Q^1) and P-O-P symmetric stretching (Q^1) [8,23].

The spectrum of glass with maximum K_2O content shows the progressive development of a new band at ~974 cm^{-1} corresponding to the symmetric stretching vibrations of P-O bonds of the orthophosphate PO_4^{3-} units (Q^0) [20]. This band is dominant bans in the spectrum while all the other bands founded under this concentration, decrease in intensity with increasing x and finally vanish.

As shown in figure 4.10 the spectrum of $0.5{\cdot}K_2O{\cdot}0.5[P_2O_5{\cdot}CaO]$ glass exhibit two broad bands (low intensity) at ~609 cm^{-1} and ~422 cm^{-1} which are assigned to the symmetric stretching of the P-O bonds and O-P-O bending modes of the orthophosphate PO_4^{3-} units(Q^0) respectively. For higher potassium oxide content it appears that, the modifier oxide (K_2O) favors the presence of O-P-O bending modes and symmetric stretching of P-O-, information revealed by bands from ~ 452 cm^{-1} and ~561 cm^{-1}. And also at this concentration appear for high wavenumber band from ~ 1093 cm^{-1} assigned to the asymmetric vibrations of $(PO_3)^{2-}$ from end of phosphate chains [21-26].

All these variations in the Raman spectra suggest a change in the covalent character between P and O bonds, that is induce by the presence in calcium phosphate glasses structure of potassium cations.

For x=20 and 35%mol studied glasses present the most high grad of disorder as can be observed in Raman spectra.

Table 4.5. Raman bands assignments for $xK_2O{\cdot}(100\text{-}x)[P_2O_5{\cdot}CaO]$ glass system, $0 \leq x \leq 50$mol%.

ν (**(**cm^{-1})	Attribution
~340	$(PO_2)^-$ of the Q^2 species and chain O-P-O bending vibrations
~422	Bending vibrations of O-P-O from Q^0 units
~452	Bending vibrations of O-P-O
~540	Symmetric stretching of P-O- bonds and O-P-O bending modes
~561	Symmetric stretching of P-O- bonds
~609	Symmetric stretching of the P-O- bonds
~700	Asymmetric stretching vibrations of P-O-P linkages in Q^2 and Q^1 structural units
~762	P-O-P symmetric stretching in Q^1 units
~974	Symmetric stretching vibrations of P-O bonds of the PO_4^{3-} (Q^0)
~1030	P_2O_7 groups $\gamma_s(PO_3^{2-})$
~1044	Symmetric stretching vibrations of $(PO_3)^{2-}$ (Q^1)
~1093	Asymmetric vibrations of $(PO_3)^{2-}$ from end of phosphate chains
~1162	Symmetric and asymmetric stretching vibrations of $(PO_2)^-$ groups from Q^2 units
~1250	Vibrations of P=O bonds existed in Q^2 units

4.3 Structural characterization of $xAu_2O_3 \cdot (100-x)[P_2O_5 \cdot CaO]$glass system

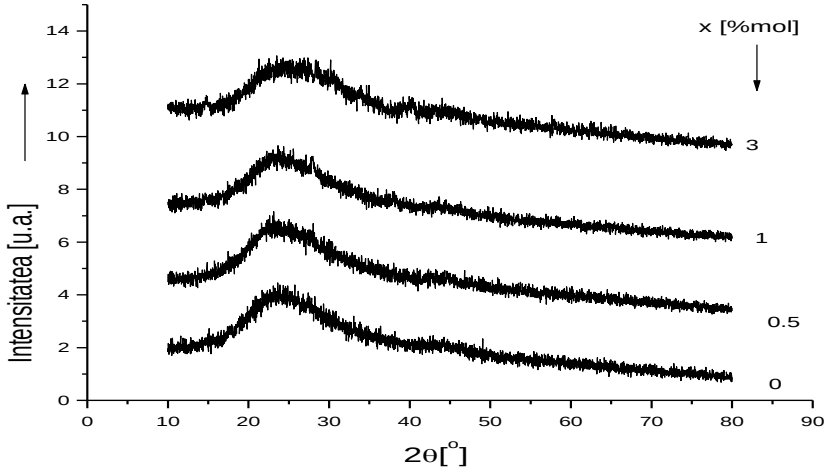

Fig. 4.11 X-ray diffractograms of
$xAu_2O_3 \cdot (100-x)[P_2O_5 \cdot CaO]$ glass system

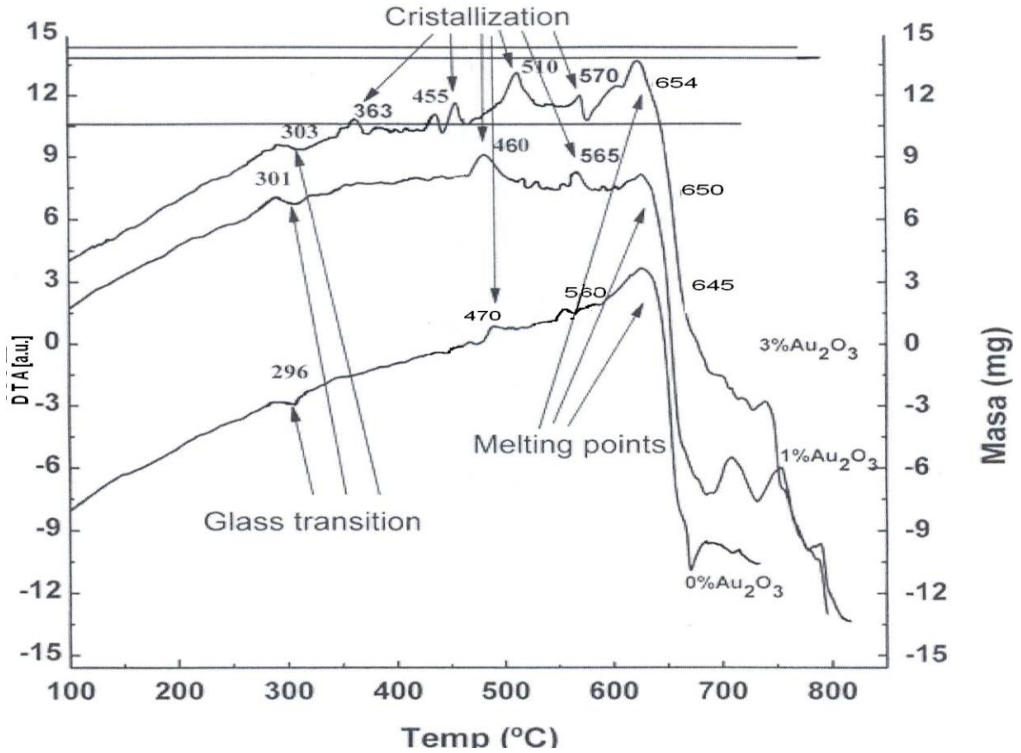

Fig. 4.12 DTA and TGA of $xAu_2O_3 \cdot (100-x)[P_2O_5 \cdot CaO]$glass system, cu x=0; 1 and 3%mol

(Tc): 460˚C; 565˚C for x=1%mol ; 363˚C; 455˚C; 510˚C; and 570˚C for x=3%mol;

(Tm): 650˚C for x=1%mol; 654˚C for x=3%mol.

The features of the DTA lines do not permit clearly to specify the glass transition temperature Tg (which is the onset of the endothermic peak) for all three samples, but the bottom curves in Fig.4.12 indicates that this temperature should be at about 296˚C for P2O5·CaO, 301˚C for $1Au_2O_3$ ·99[P_2O_5· CaO] and 303˚C for $3Au_2O_3$ ·97[P_2O_5·CaO] .

From DTA lines it is also possible to determine the crystallization temperature T_C. For glass matrix case we observe a well definite exothermic peak at 470˚C and another at 560˚C as a result of the formation of crystalline phases during the heating.

To note that Tg and Tm increase with gold oxide content: Tg 296→301; 303˚C and Tm 638→641; 645. This phenomenon can be explained by the fact that gold has a big melting point (1064.18 °C) compared to phosphorus (280.5˚C) and calcium (842˚C). With the introduction of gold oxide in glass matrix increases the amount of gold atoms at the expense of calcium and phosphorous.

The thermal stability of the same three samples was also investigated by Thermo gravimetric analysis (TGA) measurements. Thermal gravimetric analysis was used to measure the losses of weight as the temperature of the samples is increased. TGA curves glass samples are shown in Fig. 3. The TGA curves are constant for all samples m1= 10,05mg (x=0); m2=13,73mg (x=1) and m3=14,59mg (x=3) during the heating process. No weight loss of mass was observed in any studied samples for their temperature range between 100 and 850˚C.

The infrared absorption spectra obtained for the xAu_2O_3·(100-x)[P_2O_5 ·CaO] glasses with $0 \leq x \leq 3$ mol% are present in figure 4.13. The spectra reflect the minor structural rearrangements of different phosphate structural groups. These groups may connect in several ways increasing the number of allowed vibration modes.

IR analyses spectra reveal that the low frequency envelope around 500cm^{-1} consists of tow component bands at ~495 and ~536 cm^{-1}. The band about 495 cm^{-1} is assigned as the bending vibrations of P-O-P units, δ(PO_2) modes of (PO_2^-)n chain groups, and the band at ~536 cm^{-1} is described as a fundamental frequency of (PO_4^{3-}) or as harmonics of P=O bending vibration. The large band 720- 775 cm^{-1} is attributed to a P-O-P stretching vibrations from Q^2 units [3, 4, 27].

The absorption band at ~ 920 cm^{-1} is attributed to asymmetric stretching vibration of P-O-P groups linked with linear metaphosphate chain. The variation of the frequency of P-O-P bonds with increasing Au_2O_3 content shows the breakage of cyclic P-O-P bonds in the glass when the gold oxide acts as a network modifier and intensity of band rise to a maxim for x=3%mol.

It has been suggested that the band at the highest wave number ~ 1279cm^{-1} is caused by the P=O double stretching bond from Q^2 species. The band at ~1120 cm^{-1} is due to PO_3^{2-} asymmetric and symmetric vibrations (Q^1) [3-5]. This band increase in its relative area with increasing of gold oxide concentration, it may be considered as an indication for the formation of more terminal phosphate groups, PO_3^{2-}.

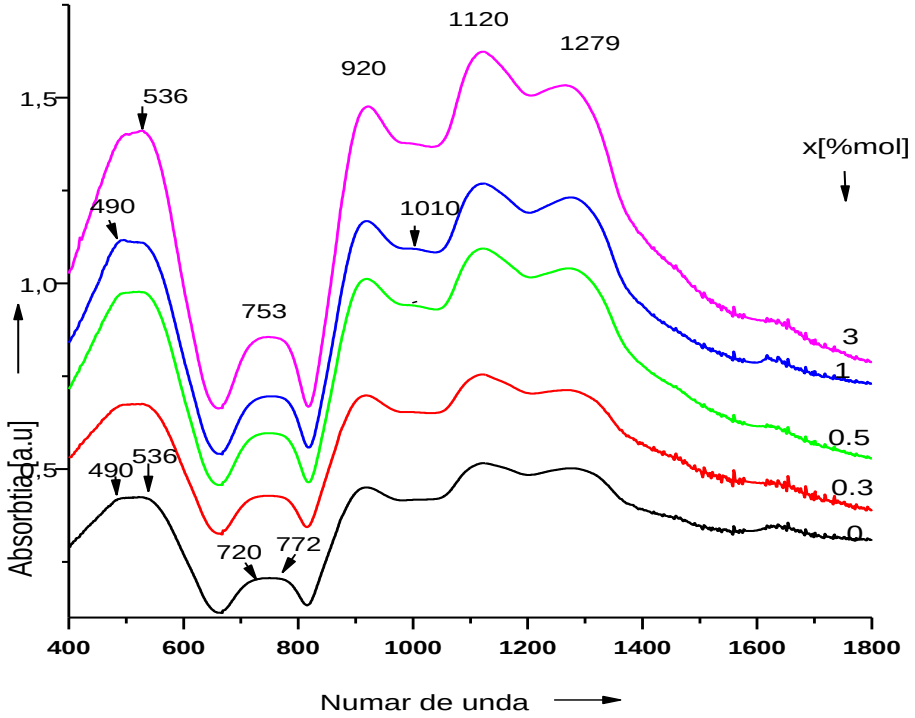

Fig. 4.13 FT-IR spectra of x Au_2O_3·(100-x)[P_2O_5· CaO] glass system, 0≤x≤3 %mol

Adding gradually small quantities of gold oxide in to the glass matrix composition induces no major changes in term of line shape. For x>0.5%mol appears a little new band at ~1010cm^{-1} characteristic for symmetric stretching of $P\text{-}O^-$ bonds in the $(PO_3)^{2-}$ end groups. Changes with the addition of gold oxide are present only in the 840-1380cm-1 range, involving the evolution of the intensity and relative area under the absorption bands in this wavenumber domain. The analysis of this spectra region revealed that the amount of P – O – P bonds bridging with rings structures (912cm-1) increases with mol%Au_2O_3 content.

This means that for higher content of gold oxide the ring type structure breaks into short arrangements such a small metaphosphate chain evidenced in spectra by the increases in intensity of the bands from 912 to 920cm-1.

Figure 4.15 shows the Raman spectra for all investigated glasses. For [P_2O_5·CaO] glass matrix spectrum presents the follow seven bands: ~334 cm^{-1}, ~534 cm^{-1}, 611 cm^{-1}, 706 cm^{-1}, 1019 cm^{-1}, ~1162 cm^{-1} and ~1255 cm^{-1}. These bands are present in majority of lines spectra; it can be explained by little content of gold oxide comparative with content of P_2O_5-CaO glass matrix.

The most intense bands from Raman spectra at ~1162 cm^{-1} has attributed to the symmetric and asymmetric stretching vibrations of $(PO_2)^-$ groups from Q^2 units, respectively band from ~706 cm^{-1} was assigned to the asymmetric stretching vibrations of P-O-P linkages in Q^2 and Q^1 structural units. The shoulder exhibits at ~ 611cm^{-1} corresponds to symmetric stretching of the P-O- bonds of the orthophosphate PO_4^{3-} units(Q^0) [27-30].

First band presented in spectrum at ~334 cm^{-1} is attributed to skeletal deformation vibration of phosphate chain and PO_3 deformation vibrations of pyrophosphate segments [28].

The large band situated at 450-570 cm^{-1}, with maxim at ~534cm^{-1}, associated with phosphate polyhedral is well observed only for glass matrix and x=0.5mol%, corresponds to the symmetric stretching of P-O- bonds and O-P-O bending modes [31].

Other bands (two shoulders) appear at ~ 1019 cm^{-1} typical of P_2O_7 group with $\gamma_s(PO_3^{2-})$ and ~1255 cm^{-1} due to the asymmetric vibrations of P=O bonds existed in Q^2 groups [28, 29].

As shown in figure 4.15 for x ≥ 0.3%mol line spectra exhibits one broad band, low intensity, at ~392cm^{-1} which are assigned to the symmetric stretching of the P-O bonds and P-O-P bending modes of the orthophosphate PO_4^{3-} units (Q^0) [32-35].

For 1-3mol% quantity of gold oxide in glass matrix composition shows the beginning of a new low band at ~912 cm^{-1} attributed to asymmetric and symmetric stretching vibrations of P-O-P linkages.

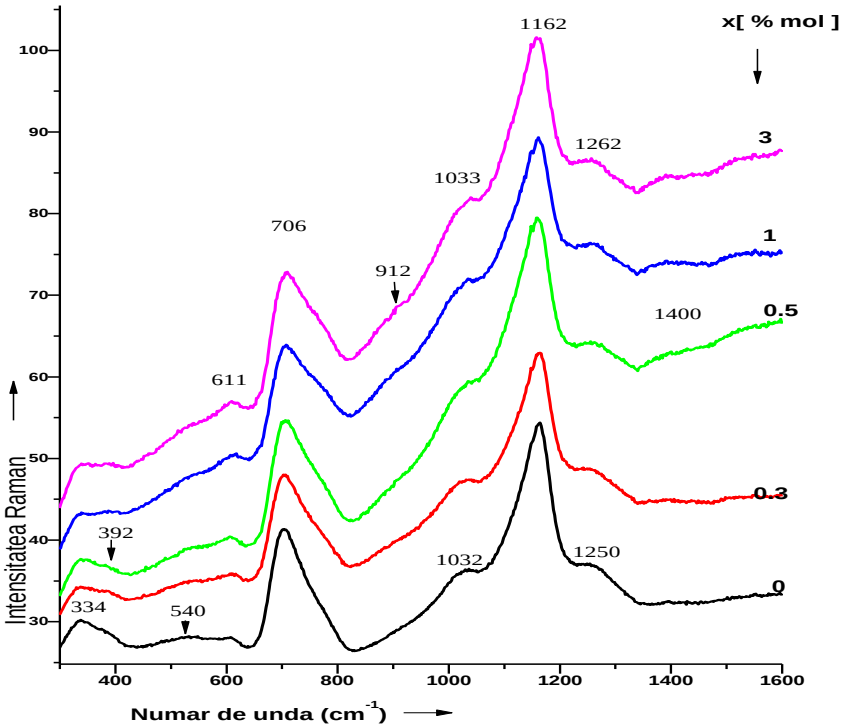

Fig. 4.15 Raman spectra of $xAu_2O_3 \cdot (100-x)[P_2O_5CaO]$glass system, $0 \leq x \leq 3$ %mol

4.4. Results obtained after immersion of glass sample in simulated body fluid

Additional evidence for the formation of crystalline phases on the surface of glass after the immersion in SBF was also obtained by SEM analyses of the samples.

The recent increased research activity in soft and hard tissue engineering, for improved tissue generation, has accentuated the need for biodegradable materials having the potential of a specific and controllable bioactivity [36]. Bioactive ceramic, particularly those derived from precursors including P_2O_5, have been the subject of extreme interest for the last 30 years. These were studied as materials for tissue repair and regeneration purposes as these compounds. When exposed bioactive glasses and ceramic to physiological fluids in vivo it have been shown to support the formation of bone mineral layer on their surface. It has been demonstrated that this mineralized layer has the capacity to bond to collagen synthesized by the cells of the connective tissue [37].

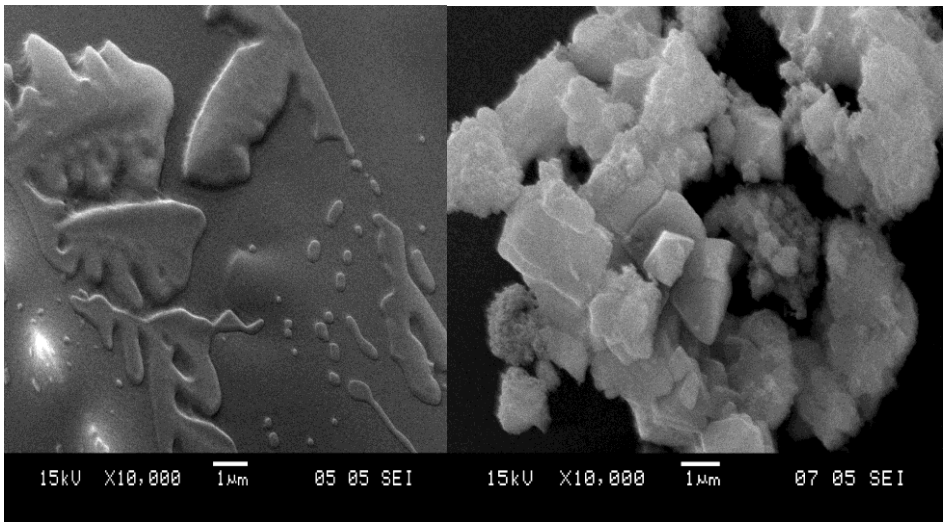

Fig. 4.16 SEM micrographs of $[P_2O_5 \cdot CaO]$ before and after immersion in SBF for 28 days

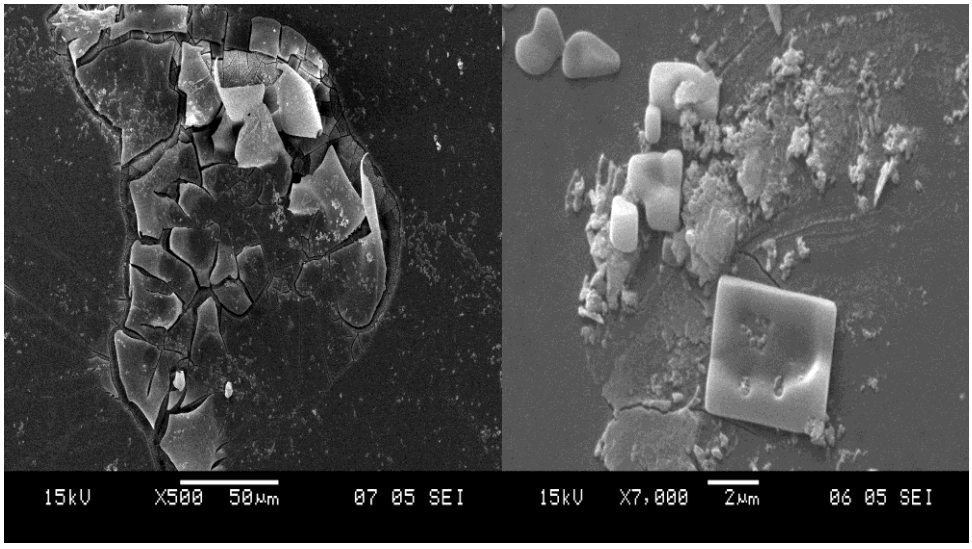

Fig. 4.17 SEM micrographs of glass $xAg_2O \cdot (100-x)[P_2O_5 \cdot CaO]$ with x=0.5 and 1%mol ;

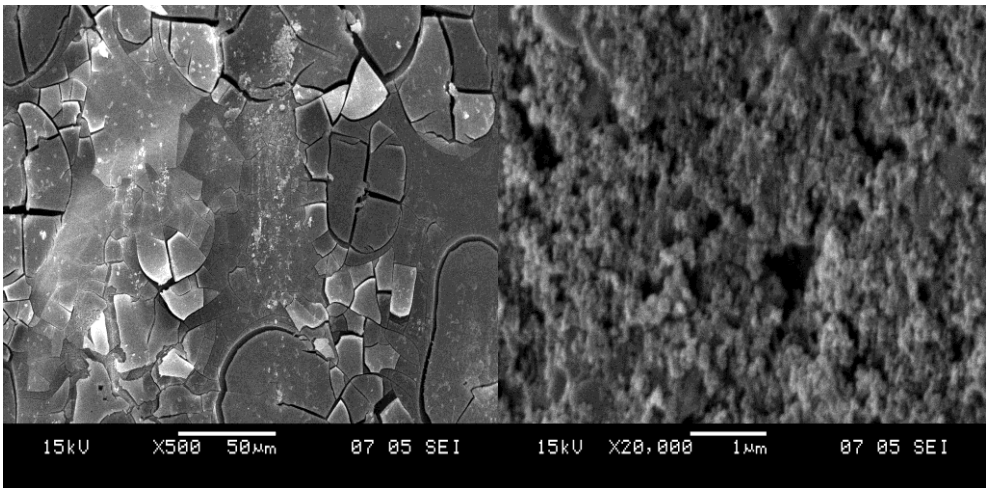

Fig. 4.18 SEM micrographs of glass $xK_2O\cdot(100-x)[P_2O_5\cdot CaO]$ with x=1 and 20%mol;

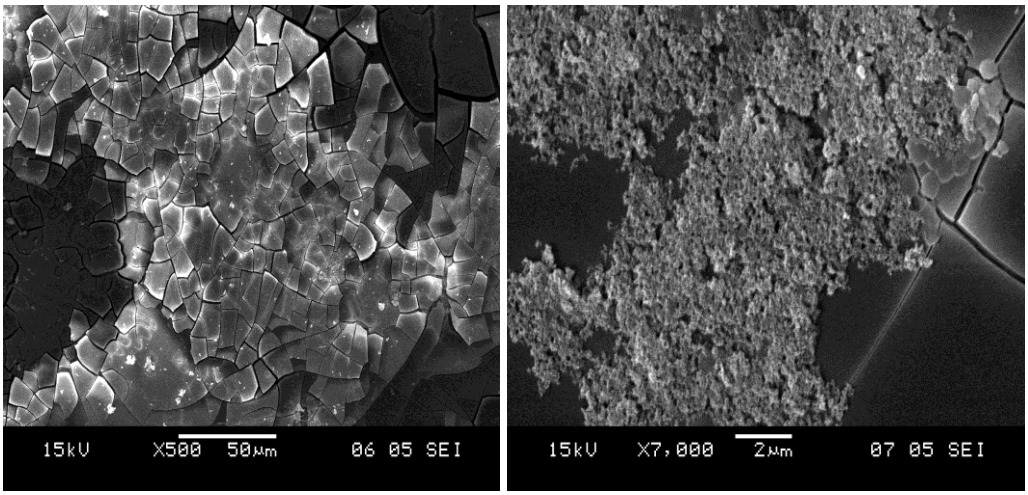

Fig. 4.19 SEM micrographs of glass $xAu_2O_3\cdot(100-x)[P_2O_5\cdot CaO]$, x=0.5 and x= 3%mol;

Figures 4.17-4.19 show well observed particles agglomerate into micro aggregates, from scanning electron micrographs of the surface of glasses samples recorded after immersion in simulated body fluid for 28 days.

The effect of SBF soaking induces structural changes on the surface, reflected by the appearance of nano-crystalline particles agglomerated into micro aggregates (fig.4.18). This apatite formation is one of an indication for the bioactivity of these materials. The mechanism of apatite formation may be explained by initial dissolution of Ca^{2+} and phosphorous ions from the surface of the bioactive glass [13, 26] with increase the degree of super saturation of the surrounding fluid, resulting in precipitation of new apatite crystal on the surface of the glass.

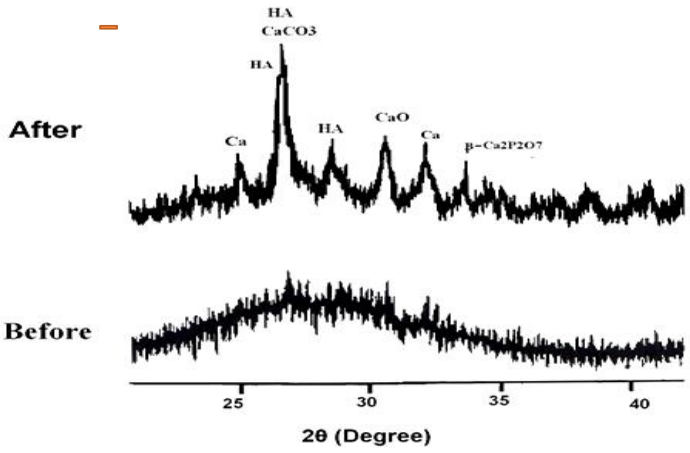

Fig. 4.20 X-ray difractograms obtained after imersion of powder sample $1Ag_2O \cdot 99[P_2O_5 \cdot CaO]$ in SBF after 28 days

4.5. Rezults obtained on glass samples after antibacterial tests

In frist part was tested glass samples and then powder of this glasses

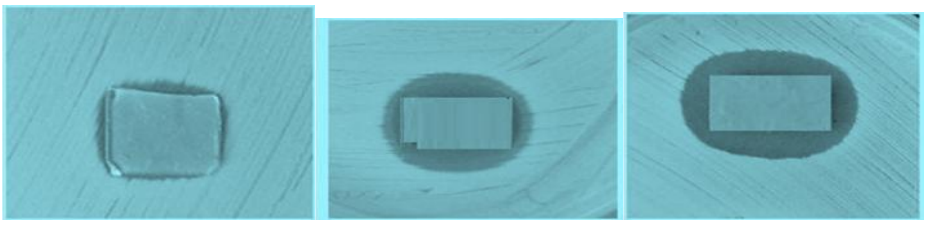

Fig. 4.23 Glass samples from $xAg_2O(100-x)[P_2O_5CaO]$, with x=0.5; 1, 5%mol on Salmonella

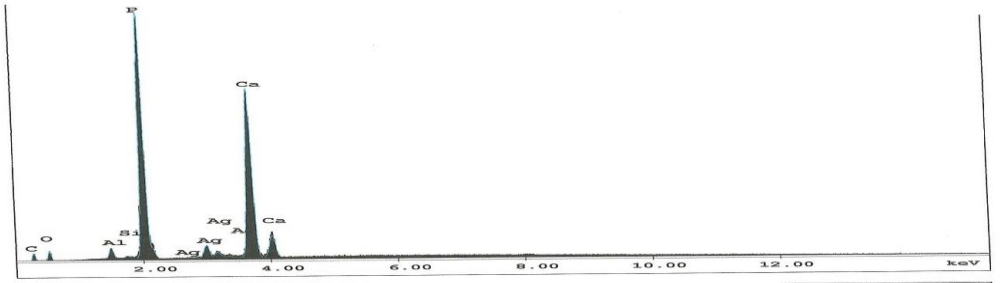

EDAX ZAF Quantification (Standardless)
Element Normalized
SEC Table : Default

Element	Wt %	At %	K-Ratio	Z	A	F
C K	12.32	26.99	0.0169	1.0673	0.1282	1.0004
O K	11.07	18.22	0.0110	1.0522	0.0941	1.0003
AlK	1.76	1.72	0.0087	0.9852	0.4944	1.0159
SiK	0.33	0.31	0.0021	1.0149	0.6128	1.0286
P K	33.04	28.08	0.2419	0.9821	0.7374	1.0109
AgL	6.22	1.52	0.0482	0.8212	0.9151	1.0308
CaK	35.26	23.16	0.2747	0.9914	0.7858	1.0000
Total	100.00	100.00				

Fig. 4.25 b) EDX spectra of powder samples $5Ag_2O \cdot 95\ [P_2O_5 \cdot CaO]$

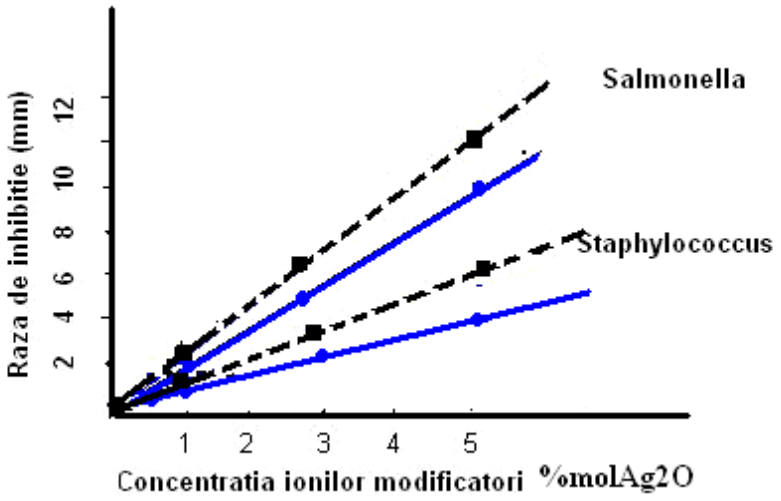

Fig. 4.26 Dependence of the radius of inhibition and concentration of silver ions $xAg_2O\cdot(100-x)[P_2O_5\cdot CaO]$, ----- powder samples, — glass samples

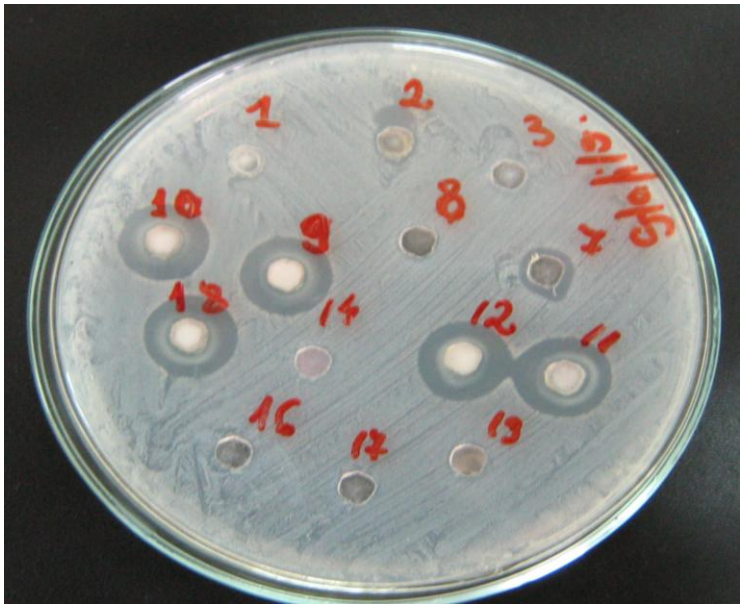

Fig. 4.27 Inhibition zone on Staphylococcus for powder samples

Fig. 4.28 Inhibition zone on Salmonella for powder samples

9- $0{,}3Ag_2O{\cdot}99{,}7{\cdot}[P_2O_5{\cdot}\ CaO]$;

10- $0{,}5Ag_2O{\cdot}99{,}5P_2O_5{\cdot}\ CaO]$;

11 - $1Ag_2O{\cdot}99{\cdot}[P_2O_5{\cdot}\ CaO]$;

12 - $5Ag_2O{\cdot}95{\cdot}[P_2O_5{\cdot}\ CaO]$.

Also was antibacterial tested distillate water were was put glass samples/ powder samples with silver oxide for 78h.

In conclusion was demonstrated antibacterian efect of glasses from $xAg_2O{\cdot}\ (100\text{-}x)[P_2O_5{\cdot}CaO]$ system.

Selective reference

[I.38] I. D. Xynos, A. I. Edgar, L. D. K. Buttery, L. L. Hench, J. M. Polak, J. Biomed. Mater. Res, 55, 151 (2001)

[I.39] L. L. Hench, D. E. Day, W. Holand, V. M. Rheinberger, Glass and Medicine**,** Int. J. Appl. Glass Sci; 1:104, (2010)

[I.40] J. K. Bibby, N. L. Bubb, D. J. Wood, P. M. Mummery, J Mater Sci: Mater. Med; 16:379, (2005).

[II.1] E. Lippama, M. Magi, A. Samoson, G. Enghelhardt, A. R. Grimmer, J. Am. Chem. Soc., 102, 4889 (1980)

[II.2] J.R. Van Wazer, Phosphorus and its Compounds, Interscience Publishers Ltd.London, 1958

[II.3] Y. M. Moustafa , K. E.Egili , J. Non–Cryst. Solids, 240, 144 (2003)

[IV.4] R. Ciceo Lucacel, I. Ardelean, **A. Regos**, Fifth General Conference of the Balkan Physical Union BPU5, August 25-29, 2003, Book of abstracts,p.112

[IV.5] J. M. Arzeian and C. A. Hogarth , J. Mater. Sci., 26 (19), 5353 (1991)

[IV.6] M. A. Salim, G. D. Khattak, P. S. Fodor, L. E. Wenger, J. Non–Cryst. Solids, 299, 185 (2001)

[IV.13] J. Sun, Li Yongsheng, Liang Li, W. Zhao, Lei Li, J. Gao, M.Ruan, J.Shi, J. Non–Cryst. Solids, 354, 3799 (2008)

[IV.16] N.Vedeanu, O. Cozar, I. Ardelean, S. Filip, J. Optoelectron. Adv. Mat., 8, 1135 (2006)

[IV17] D. Di Martino, L.F. Santos, A.C. Marques, R.M. Almeida, J. Non-Cryst. Solids, 293, 349 (2001)

[IV.21] R. Ciceo Lucacel, A.O.Hulpus, V. Simion, I. Ardelean, J. Non–Cryst. Solids, 355, 425 (2009)

[IV.22] J. Garbarczyk, P. Machowski, M. Wasincionek, L.Tykars, R.Bacewicz, A.Aleksiejuk, Sol. State Ionics, 136 , 1077 (2000)

[IV.23] M. A. Karakassides, A. Saranti , I. Koutselas, J. Non–Cryst. Solids, 347, 69 (2004)

[IV.24] G. Le Ssaout, P. Simon, F. Fayon, A. Blin, Y. Vaills, J. Raman Spectrosc., 33, 740 (2002)

[IV.46] **A. Regos** R. Ciceo Lucacel and I. Ardelean, J. Mater. Sci., 46, 22, p. 7313 (2011)

[IV.48] P. Dibrov *et al.* Antimicrobial Agents and Chemotherapy, 46, 8, 2668 (2002)

[IV.49] R.Cooper, A. Review of the Evidence for the use of Topical Antimicrobial Agents in Wound Care, World Wide Wounds, 2004

[IV.50] **A. Regos,** I. Ardelean, J. Mol. Struct., 1006, 1, p. 312 (2011)

Selective conclusions

●Were prepared glasses from systems $xAg_2O\cdot(100-x)[P_2O_5\cdot CaO]$; $xK_2O\cdot(100-x)[P_2O_5\cdot CaO]$; $xAu_2O_3\cdot(100-x)[P_2O_5\cdot CaO]$;

● For a comparative study of the structure of these glass samples wereprepared in the same conditions (furnace, crucibles, melting and equilibriumtemperatures during melting;

- X-ray diffractograms of $xAg_2O\cdot(100-x)[P_2O_5\cdot CaO]$ show that these are vitreus under 5%mol;
- The differential thermal analysis - (Tg) increases with increasing its content from 295 ˚ C (0%molAg2O) to 299 ˚ C (1% molAg2O) at 303 ˚ C (3% molAg2O). At the same time and crystallization temperature (Tc) changes from 470 ˚ C (500 ˚C) → 560 ˚ C (580 ˚ C) → 587 ˚ C (586 ˚ C) signifying crystallization of twophases. Also the melting temperature (Tm) increases with increasing content of silver oxide to 645 ˚ C (0 mol% Ag2O) → 648 ˚ C (1%molAg2O) → 655 ˚ C (3% molAg2O). ATGcurves show that mass does not vary in the range studied, so the samples do not contain water onother volatile materials were evaporated with increasing temperature;

- . Raman spectra of glasses in the study of system xAg2O • (100-x) [P2O5• CaO] can be observed that samples studied represents only specificbands of different vibrations phosphatic units, whose content varies with increasing Ag2O content;

- X-ray diffractograms of $xK_2O\cdot(100-x)[P_2O_5\cdot CaO]$ show that these are vitreus under 50%mol ;
- IR absorption spectra indicate the presence of different phosphategroups whose concentration varies with K_2O content. Major changes arenoted at concentrations above 35 mol% K2O. Since this concentrationstands out clearly in the 400-600 cm-1 two new bands at ~ 490 cm-1 and 596 cm-1 corresponding to the formation of ionic groups and $P_2O_7^{4-}$,PO_4^{3-}due to breakage of bonds;

- Study Raman spectra of glasses in the system xK2O • (100-x) [P2O5CaO] showed that significant changes occur depending on the proportion of K_2O. Raman spectra indicate that the disordered glasses are obtained for x = 20% and 35 mol% K2O;

- The melting temperature (Tm) is situated at 645 ˚ C (0 mol% Au2O3) 650 ˚ C (1% mol Au2O3) and 654 ˚ C (3% mol Au2O3). From these resultsit is noticed that the gold ions is more significant crystallization agent than silver and potassium ions. Neither phosphate glasses in this system there was no mass loss with increasing temperature.
- After immersion in simulated body fluid massive glasses for a period of 28 days at 37 ˚ C, show the formation of hydroxyapatite on their surfaces. The immersion was followed by baleaj electron microscopy, SEM. SEM images obtained after 28 days shows exintens of new formations from surface samples. X-ray difractograms performed on powde rsamples after 28 days, showed the presence of crystalline structures corresponding hidroxyapatite, calcium carbonate and calcium. This hydroxyapatite on the surface of glass samples after the introduction of afluid whose composition is similar to human plasma is a first indication of the bioactivity of these materiale.

● The results of antibacterial tests of glasses studied (tests were performed with Salmonella and Staphylococcus bacteria) have shown that pieces of glass in their composition Ag_2O they are more efficient, with increasing the concentration of silver ions. Samples containing K_2O and Au_2O_3 not block bacterial growth and therefore fail to cure infections with Salmonella or Staphylococcus